Radiative and Nonradiative Transitions in the Fluorescence Decay of Eu3+ in SrTiO3

M. J. Weber and R. F. Schaufele

Citation: The Journal of Chemical Physics **43**, 1702 (1965); doi: 10.1063/1.1696994
View online: http://dx.doi.org/10.1063/1.1696994
View Table of Contents: http://scitation.aip.org/content/aip/journal/jcp/43/5?ver=pdfcov
Published by the AIP Publishing

Radiative and Nonradiative Transitions in the Fluorescence Decay of Eu^{3+} in $SrTiO_3$

M. J. Weber and R. F. Schaufele
Raytheon Research Division, Waltham, Massachusetts

(Received 26 April 1965)

The fluorescence excitation and decay properties of Eu^{3+} in $SrTiO_3$ have been studied using steady-state and pulse techniques. The transient fluorescence response following pulsed selective excitation was used to establish the modes of energy decay. The probabilities for spontaneous magnetic-dipole emission were calculated for several states. These results combined with relative fluorescence intensity measurements are compared with the observed fluorescence lifetimes to determine the probabilities for radiative and nonradiative decay. Whereas the decay of the $^5D_0$ state is radiative, consisting of both zero-phonon and phonon-assisted transitions, the $^5D_1$ decay is composed of radiative transitions to states of ^7F and nonradiative transitions to $^5D_0$, the latter being dominant. The $^5D_0$ and $^5D_1$ fluorescence lifetimes exhibit different temperature dependences which are discussed in terms of the contributions from phonon-assisted and multiphonon nonradiative transitions. The change in the $^5D_0$ lifetime as the temperature is varied through the 110°K phase transition of $SrTiO_3$ is $\lesssim 10\%$.

INTRODUCTION

RADIATIVE, phonon-assisted, and nonradiative transitions may contribute to the decay of excited paramagnetic ions in solids. All of these processes are active between various energy levels of trivalent europium in strontium titanate. To determine the modes of energy cascade and the rates, relative importance, and temperature dependences of the above processes in this crystal, the steady-state and transient fluorescence excitation and decay properties were investigated. The general approach is one used several years ago by Rinck[1] in studying the radiative and nonradiative processes in another europic salt. The probability for spontaneous emission from an excited state to the ground state, determined either from the corresponding integrated absorption coefficient and use of the relationship between the Einstein A and B coefficients[2] or from theoretical calculation, is combined with the observed relative intensities of fluorescence transitions to other terminal states to find the total radiative lifetime. This is then compared with the measured excited-state lifetime, any difference being attributed to the presence of nonradiative transitions.

The $SrTiO_3$ host has the cubic perovskite structure above 110°K. If rare-earth ions enter this lattice substitutionally at cubic crystal-field sites, electric-dipole transitions between states of the ground $4f^n$ configuration are forbidden by Laporte's rule. Magnetic-dipole transitions, however, are allowed. Recently, Axe[3] examined the radiative transition probabilities within $4f^n$ configurations and the $4f^6$ configuration of Eu^{3+} in europium ethylsulfate in particular. His success in obtaining agreement between observed and predicted relative fluorescence intensities lends confidence to calculations of the probabilities for spontaneous magnetic-dipole emission. This is important in the present case since the absorptive transitions required for an experimental determination of these probabilities were too weak to be observed.

After a discussion of the fluorescence spectrum and modes of excitation and energy cascade within the energy-level system of Eu^{3+} in $SrTiO_3$, a comparison is made between the predicted radiative lifetime, using theoretical calculations of the magnetic-dipole probabilities, and the observed fluorescence lifetime of the $^5D_0$ and $^5D_1$ states. Radiative processes are considered herein to include both zero-phonon and phonon-assisted transitions, their relative importance being evident from their respective intensities in the over-all fluorescence spectrum. The spectrum and interpretation of phonon-assisted transitions present in $SrTiO_3$: Eu^{3+} have been discussed previously[4] and provide information about the lattice vibrational frequency spectrum of $SrTiO_3$.

FLUORESCENCE SPECTRUM

Trivalent Eu has a $4f^6$ rare-earth electronic configuration. The free-ion energy levels have been calculated recently by Ofelt[5]; the lower energy levels, which are of interest for this investigation and account for the general features of the observed spectra, are shown in Fig. 1. Fluorescence has been observed from the $^5D_0$ and $^5D_1$ states of Eu^{3+} in $SrTiO_3$ to levels of the ^7F ground term. The terminal levels and wavelengths of several of the more intense fluorescence lines at 77°K are given in Table I. The assignments are based upon the correspondence with wavelengths of fluorescence lines of Eu^{3+} in other hosts.[6] Since the lifetimes of the two fluorescent states differ by one order of magnitude, the lifetimes of individual lines

[1] B. Rinck, Z. Naturforsch. **3**, 406 (1948).
[2] See, for example, the discussion by D. L. Dexter in Solid State Phys. **6**, 353 (1958).
[3] J. D. Axe, Jr., J. Chem. Phys. **39**, 1154 (1963).
[4] M. J. Weber and R. F. Schaufele, Phys. Rev. **138**, A1544 (1965).
[5] G. S. Ofelt, J. Chem. Phys. **38**, 2171 (1963).
[6] N. C. Chang, J. Appl. Phys. **34**, 3500 (1963); N. C. Chang and J. B. Gruber, J. Chem. Phys. **41**, 3227 (1964); E. V. Sayre and S. Freed, *ibid.* **24**, 1213 (1956); L. G. DeShazer and G. H. Dieke, *ibid.* **38**, 2190 (1963).

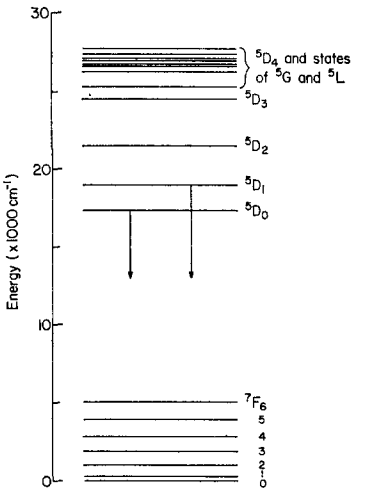

FIG. 1. Lower energy levels of Eu^{3+} (crystal-field splittings are not shown). Fluorescence is observed from $^5D_0$ and $^5D_1$ to levels of ^7F for $SrTiO_3$:Eu^{3+}.

were examined to identify the upper states. No emission from $^5D_2$ or higher electronic states was noted.

Although several weaker fluorescence lines were observed, which are not included in Table I, all lines expected from the crystal-field splitting of the J degeneracies in either a cubic or lower symmetry field (see Appendix) were not observed or not properly identified. Difficulties in assigning lines arose from the presence of both zero-phonon and phonon-assisted lines, the proximity or overlapping of groups of lines from different excited states, and their low intensity. Also, in cubic symmetry there is no polarized spectrum to aid in the identification of transitions. Estimates of the crystal-field parameters for $SrTiO_3$:Eu^{3+} were not considered warranted with the present data. Since no splitting of the $^5D_1$ or $^7F_1$ states was detected[4] at 77°K, noncubic crystal-field components appearing below the 110°K phase transition are probably small.

Fluorescence was excited by pumping ions into a broad excitation band extending from approximately 24 500 to 29 000 cm^{-1} which consists principally of closely spaced states of ^5D, ^5G, and ^5L. The $^5D_0$ fluorescence could also be excited by pumping directly into $^5D_1$ and $^5D_2$; however, the resulting fluorescence was very much weaker. Attempts to observe corresponding transitions in the absorption spectrum of our samples of $SrTiO_3$:Eu^{3+} were unsuccessful.[4]

TABLE I. Wavelengths of principal fluorescence lines from the $^5D_0$ and $^5D_1$ levels of Eu^{3+} in $SrTiO_3$ at 77°K.[a]

Lower state for fluorescence	$^5D_0$	$^5D_1$
$^7F_0$	5779 Å	5256 Å
$^7F_1$	5910	5364*
$^7F_2$	6152*	5549, 5570
$^7F_3$	~6500	5820
$^7F_4$	6840, 6903* 7012, 7055	(6120–6300)
$^7F_5$	~7500	(~6650)
$^7F_6$	~8200–8300	(~7200)

[a] Wavelengths in parentheses are predicted. An asterisk denotes lines which appear or increase in intensity below 110°K.

TABLE II. Relative intensities of fluorescence transitions from the $^5D_0$ state of Eu^{3+} in $SrTiO_3$. Results are normalized to the $^5D_0 \rightarrow {}^7F_1$ intensity at each temperature.

Transition	Relative fluorescence intensity 80°K	160°K	295°K
$^5D_0 \rightarrow {}^7F_0$	0.01	0.02	0.03
$^5D_0 \rightarrow {}^7F_1$	1.00	1.00	1.00
$^5D_0 \rightarrow {}^7F_2$	1.49	1.10	1.28
$^5D_0 \rightarrow {}^7F_3$			0.03
$^5D_0 \rightarrow {}^7F_4$	1.45		2.5
$^5D_0 \rightarrow {}^7F_5$			~0.02
$^5D_0 \rightarrow {}^7F_6$	$\lesssim$0.3		0.96

The relative intensities of fluorescence transitions from $^5D_0$ and $^5D_1$ are recorded in Tables II and III, respectively. The intensities are given in terms of the relative number of photons and include any vibrational sidebands associated with the transition. Data were recorded using a 0.5-m Bausch & Lomb grating monochromator and a liquid-nitrogen-cooled RCA-7102 photomultiplier. Correction was made for the spectral response of the over-all detection system, arising principally from the variation of the photomultiplier sensitivity and grating efficiency with wavelength, by calibrating it using a source of known spectral intensity. The estimated uncertainties in the intensity measurements range from $<10\%$ for the strongest lines to a factor of 2–3 for the weakest. The uncertainty of the $^5D_0 \rightarrow {}^7F_6$ intensity arose from the decreasing sensitivity of the over-all detection system at longer wavelengths. As can be seen from Table I, several of the longer-wavelength $^5D_1$ fluorescence transitions are predicted in the vicinity of transitions from $^5D_0$ and, if present, were comparatively weak and not resolved.

In the high-temperature cubic phase of $SrTiO_3$ only magnetic-dipole and certain phonon-assisted transitions are allowed. Zero-phonon electric-dipole transitions which require a change in parity between initial and final states are forbidden due to the inversion

TABLE III. Relative intensities at 77°K and magnetic-dipole probabilities for fluorescence transitions from the $^5D_1$ state of Eu^{3+} in $SrTiO_3$. Results are normalized to the $^5D_1 \rightarrow {}^7F_2$ intensity.

Transition	Relative intensity	Relative magnetic-dipole transition probability
$^5D_1 \rightarrow {}^7F_0$	0.10	0.139
$^5D_1 \rightarrow {}^7F_1$	0.71	0.005
$^5D_1 \rightarrow {}^7F_2$	1.00	1.000
$^5D_1 \rightarrow {}^7F_3$	1.1	

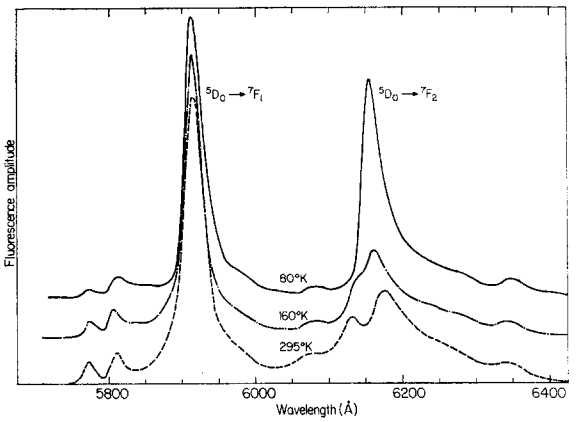

FIG. 2. A portion of the fluorescence spectrum of $SrTiO_3:Eu^{3+}$ showing the relative changes in the $^5D_0 \rightarrow {}^7F_1$ and $^5D_0 \rightarrow {}^7F_2$ transitions with temperature.

symmetry of the crystalline field. Such transitions may be allowed, however, because of lack of ideal cubic symmetry at the local Eu^{3+} impurity site. Below the 110°K cubic-to-tetragonal structural phase transition, additional lines, denoted by an asterisk in Table I, appear. This is illustrated in Fig. 2 which shows a portion of the fluorescence spectrum (low resolution) at three different temperatures. Whereas at high temperatures only the vibrational structure associated with the $^5D_0 \rightarrow {}^7F_2$ transition is evident, a zero-phonon line grows at $\approx$6150 Å in the vicinity of 110°K. (The detailed temperature dependence of this region of the fluorescence spectrum is discussed elsewhere.[4]) The $^5D_0 \rightarrow {}^7F_1$ line, on the other hand, which is predominantly an allowed magnetic-dipole transition, is relatively insensitive to temperature.

The relative intensities in Tables II and III are approximately as expected. The intensity of the $^5D_0 \rightarrow {}^7F_2$, $^7F_4$, $^7F_6$ transitions arises from vibrational interactions and crystal-field admixing of states. Since many of the reduced matrix elements for $^5D_0 \rightarrow {}^7F_6$ vanish, these lines should be weak. Also, as Ofelt[7] has pointed out, electric-dipole transitions from a $J=0$ level to an odd J level are predicted to be very weak, which is indeed observed for $^5D_0 \rightarrow {}^7F_3$, $^7F_5$. The $^5D_0 \rightarrow {}^7F_0$ line is weak since it too is a forbidden transition. Of the transitions from $^5D_1$, those to $^7F_0$, $^7F_1$, and $^7F_2$ are magnetic-dipole allowed. Their calculated relative intensities, for the zero-phonon lines, are given in the final column of Table III. The larger than expected intensity of $^5D_1 \rightarrow {}^7F_1$ is due to a combination of vibronic and zero-phonon electric-dipole transitions, the latter disappearing above 110°K in a manner similar to that of the $^5D_0 \rightarrow {}^7F_2$ transition shown in Fig. 2.

EXCITATION AND FLUORESCENCE DECAY

Fluorescence decay processes were studied by exciting the sample with a short light pulse from an FX-12 xenon flashtube. The sample, a single crystal of $SrTiO_3$ approximately $\frac{1}{8}$ in.$\times\frac{1}{8}$ in.$\times\frac{1}{2}$ in. in size doped with 0.03% Eu,[8] was contained in a quartz Dewar open at both ends through which flowed dry nitrogen gas of variable temperature. A Bausch & Lomb grating monochromator inserted between the source and the sample isolated a narrow frequency band for selective excitation experiments. The fluorescence was observed through a second grating monochromator with an RCA-7265 photomultiplier (S-20 photocathode). The transient fluorescence response was displayed on an oscilloscope. In some instances the signal-to-noise ratio was improved by continuous averaging techniques[9] using a Technical Measurements Corporation CAT-1024 digital computer. Lifetime measurements were made from photographs of the oscilloscopic presentation.

The lifetimes of the $^5D_0$ and $^5D_1$ states are plotted as a function of temperature in Fig. 3. The accuracy of individual data points for $^5D_0$ is in the order of or better than 10%. Observations of the $^5D_1$ decay were marred by the presence of light leakage from the excitation flash. This was objectionable at higher temperatures where the lifetime became comparable to the over-all system response time ($\sim$5 μsec) and hence the data in this region are corresponding more uncertain. The signal amplitudes also decreased in the higher temperature regions where the lifetimes exhibit a decrease.

The most intense fluorescence decays were obtained by excitation into the 3600–3900-Å band, the band used in the above measurements. Fluorescence decays from $^5D_0$ were also observable following direct pumping

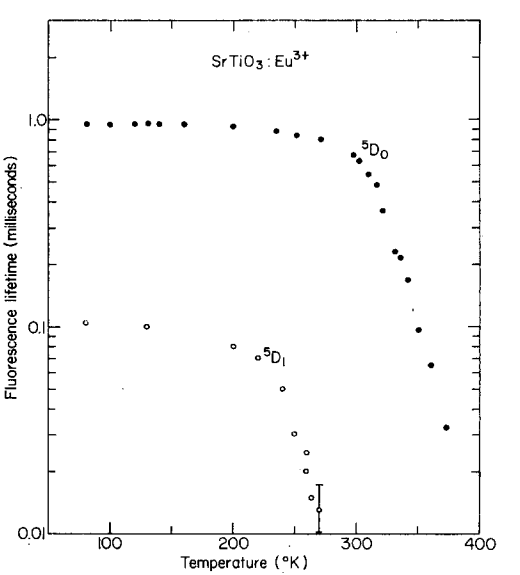

FIG. 3. Temperature dependence of the fluorescence lifetimes of the $^5D_0$ and $^5D_1$ levels of Eu^{3+} in $SrTiO_3$.

[7] G. S. Ofelt, J. Chem. Phys. **37**, 511 (1962).

[8] The $SrTiO_3:Eu^{3+}$ samples used were cut from the same boule described in Ref. 4.

[9] M. P. Klein and G. W. Barton, Jr., Rev. Sci. Instr. **34**, 754 (1963).

into $^5D_2$ and $^5D_1$ at $\approx$4600 and 5250 Å, respectively. The signals were much weaker, however, and were obtained by averaging many hundred repetitive events.

In general, the transient fluorescence from lower levels of a multilivel system such as in Fig. 1 will exhibit a time dependence composed of a linear combination of exponential terms. For example, following pulsed selective excitation into the $^5D_1$ state, the $^5D_0$ fluorescence exhibits a transient behavior made up of the difference of two exponential terms, an initial rise corresponding to the $^5D_1 \rightarrow {}^5D_0$ transition, followed by the subsequent decay of $^5D_0$ to the ^7F ground multiplet. In terms of the level lifetimes τ, the $^5D_0$ fluorescence signal is proportional to

$$\text{const.}\ \{\exp[-t/\tau(^5D_0)]-\exp[-t/\tau(^5D_1)]\}, \quad (1)$$

where the light pulse is assumed to be very much shorter than either $\tau(^5D_0)$ or $\tau(^5D_1)$. If $\tau(^5D_0)>\tau(^5D_1)$, as in the present case, the signal maximum from Eq. (1) occurs at a time

$$t_{\max}=\{\tau(^5D_0)\tau(^5D_1)/[\tau(^5D_0)-\tau(^5D_1)]\} \times \ln[\tau(^5D_0)/\tau(^5D_1)]. \quad (2)$$

Using the measured τ's at 77°K, the maximum of the $^5D_0$ fluorescence is predicted at $\approx$0.25 msec. Following excitation into $^5D_2$, the maximum is observed in the range 0.23–0.30 msec indicative of decay via $^5D_1$. The decay from $^5D_2$ into $^5D_1$ appears to be comparatively rapid, <20 μsec.

When the sample is pulse excited by radiation at 3600–3900 Å, the $^5D_0$ fluorescence maximum occurs earlier, $\approx$0.18 msec at 77°K. This is shown by the oscilloscope photograph of the time dependence of the $^5D_0$ fluorescence in Fig. 4. In addition, if the energy decay from the pump band is assumed to proceed by a step-by-step cascade via $^5D_2$–$^5D_1$–$^5D_0$, then the observed initial rise of the $^5D_0$ fluorescence is more rapid than expected from the limiting $^5D_1$ lifetime.

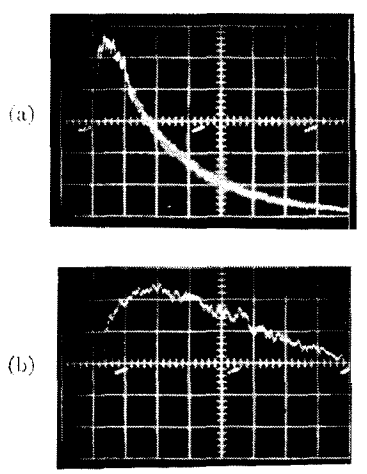

FIG. 4. Oscilloscope photograph of fluorescence from the $^5D_0$ state of Eu^{3+} in $SrTiO_3$ at 80°K following pulsed excitation at 3600 Å. Sweep rates: (a) −0.5 msec/cm, (b) −0.1 msec/cm.

The rapid rise and shifted $t_{\max}$ of the $^5D_0$ fluorescence when excited at 3600–3900 Å suggest that some of the ion population buildup in $^5D_0$ may also take place by transitions from higher levels which bypass $^5D_1$ and terminate directly at $^5D_0$. The time dependence of the $^5D_0$ population in such a case can be found by solving the rate equations for an equivalent four-level system, composed of an initial excited level E, $^5D_1$, $^5D_0$, and ^7F, in which decay from E to $^5D_0$ occurs partly by direct transitions and partly by cascade via $^5D_1$. The result is of the form

$$A\exp[-t/\tau(^5D_0)]-B\exp[-t/\tau(^5D_1)] -C\exp[-t/\tau(E)]. \quad (3)$$

Assuming $\tau(E)<\tau(^5D_1)<\tau(^5D_0)$, two terms now contribute to the initial rise of the $^5D_0$ fluorescence. Their relative importance and the location of the fluorescence maximum are dependent upon the magnitudes of the coefficients A, B, C which are functions of the various transition probabilities involved.

The initial rise of the $^5D_1$ fluorescence following excitation at 3600–3900 Å was approximately equal to that expected from the flash duration and system response time although, as noted above, it was marred by flash leakage. We estimate that the decay times of the levels which contribute significantly to the population buildup of $^5D_1$ are $\lesssim 10$ μsec.

COMPARISON OF RADIATIVE AND EXPERIMENTAL LIFETIMES

Magnetic-dipole transitions, which are well established[6] in the fluorescence spectra of Eu^{3+} in other crystals and whose strengths can be readily calculated,[3,7] are useful for relative intensity comparisons. These transitions are allowed between states of $4f^n$ subject to the selection rules ΔJ, $\Delta J_z=0, \pm 1$ and $\Delta S=\Delta L=0$. Selection rules for both electric- and magnetic-dipole transitions between crystal-field levels in $SrTiO_3$, assuming cubic and tetragonal site symmetries, are given in the Appendix. Since all lines expected in the crystal-field spectra were not identified, we consider only the total transition probabilities between crystal-field multiplets.

The probability for spontaneous emission of magnetic-dipole radiation can be calculated straightforwardly. Since we do not have sufficient information to construct appropriate crystal-field eigenstates for $SrTiO_3$:Eu^{3+}, we shall use the free-ion eigenstates derived by Ofelt[5] from diagonalization of the electrostatic and spin–orbit energy matrices. While the values of the spin–orbit parameters, Slater integrals, and the assumption of hydrogenic ratios of Slater integrals may not be exactly appropriate to $SrTiO_3$:Eu^{3+}, they should yield a reasonable description of the lower-lying excited states. The resulting eigenstates are of the form

$$|i\rangle=\sum C(i:\alpha SLJ)\ |f^n\alpha SLJ\rangle, \quad (4)$$

TABLE IV. Comparison of calculated probabilities for magnetic-dipole emission and observed fluorescence lifetime of $SrTiO_3:Eu^{3+}$ at 80°K.

Transition	Probability for magnetic-dipole emission	Magnetic-dipole radiative lifetime	Observed lifetime
$^5D_0 \rightarrow {}^7F_1$	210.8 sec^{-1}	4.75 msec	0.95 msec
$^5D_1 \rightarrow {}^7F_0$	24.4		
$\rightarrow {}^7F_1$	0.79		
$\rightarrow {}^7F_2$	175.6		
$\rightarrow {}^5D_0$	1.79		
Total	202.6	4.95	0.10
$^5D_2 \rightarrow {}^7F_1$	8.4		
$\rightarrow {}^7F_2$	0.1		
$\rightarrow {}^7F_3$	167.3		
$\rightarrow {}^5D_1$	6.9		
Total	182.7	5.47	<0.02
$^5D_3 \rightarrow {}^7F_2$	2.3		
$\rightarrow {}^7F_3$	0.09		
$\rightarrow {}^7F_4$	164.3		
$\rightarrow {}^5D_2$	9.2		
Total	176.9	5.66	

where the summation is over the quantum numbers αSL. (The SLJ labeling of states throughout this paper is that of the predominant $|f^n\alpha SLJ\rangle$ component.) The probability for spontaneous magnetic-dipole emission from State i to State j is given by

$$A_{ij}=\frac{1}{2J+1}\frac{64\pi^4\nu_{ij}^3n^3\beta^2}{3hc^3}\times\left|\sum_{\alpha SL,\alpha'S'L'}C(i{:}\alpha SLJ)C(j{:}\alpha'S'L'J')\times\langle f^n\alpha SLJ\,||\,\mathbf{L}+2\mathbf{S}\,||\,f^n\alpha'S'L'J'\rangle\right|^2. \quad (5)$$

In Eq. (5), ν_{ij} is the frequency of the transition, n is the index of refraction of the host crystal, and $\beta=eh/2mc$. Using Eq. (5) and the coefficients C given by Ofelt, the spontaneous emission probabilities from $^5D_0$, $^5D_1$, $^5D_2$, and $^5D_3$ were calculated and tabulated in Table IV. Where the exact energy of SLJ states was not known experimentally, calculated energies were used. The values of the index of refraction at various wavelengths were extrapolated from known data.[10]

The measured lifetimes of the above states of Eu^{3+} in $SrTiO_3$ at 77°K, in the region where they are temperature independent, are also given in Table IV. In all cases the zero-phonon magnetic-dipole emission probabilities alone are insufficient to account for the experimental lifetimes.

[10] *American Institute of Physics Handbook*, edited by D. Gray *et al.* (McGraw-Hill Book Company, Inc., New York, 1957).

The lifetime τ of an excited state i, however, is governed by a summation of the probabilities for radiation (R) transitions, including zero-phonon and phonon-assisted emission, and nonradiative (NR) transitions, that is,

$$1/\tau_i=\sum_j W_{i\rightarrow j}^{R}+\sum_j W_{i\rightarrow j}^{NR}, \quad (6)$$

where the summation is over all terminal states j. We shall assume that zero-phonon part of the $^5D_0 \rightarrow {}^7F_1$ transition is magnetic-dipole radiation with a probability given in Table IV. This assumption is not unreasonable in view of similar transitions observed in other crystals and the expectation that an electric-dipole transition would be weak in general and absent in cubic $SrTiO_3$. The vibrational sidebands of this transition are ≈ 0.6 times as intense as the zero-phonon line[11] at 77°K. Combining these values with the relative intensity measurements in Table II yields a total radiative probability of 1435 sec^{-1} or a radiative lifetime of 0.7 msec. The measured $^5D_0$ lifetime at 77°K is 0.95 msec. Because the Eu^{3+} content, $\lesssim 0.03\%$, and the absorption cross section for $^7F \rightarrow {}^5D_0$ transitions are both small, any lengthening of the fluorescence lifetime due to resonant self-absorption[12] should be negligible.

The observed $^5D_0$ lifetime appears, within estimated error, to be accounted for by radiative processes, thus, the presence of additional nonradiative transitions to states of ^7F_J is not indicated. Because of the large energy to be conserved in a multiphonon process and the absence of levels suitable for resonant transfer of energy by ion–ion interactions,[13] such nonradiative processes are not expected to be important.

Among possible sources of the discrepancy between the observed and predicted $^5D_0$ lifetimes are the overall accuracy of the intensity measurements and the use of general free-ion wavefunctions. The calculated magnetic-dipole probabilities are dependent upon spin–orbit admixing of states of ^5D and ^7F and hence upon the values of the parameters used in deriving the wavefunctions. Also, effects of crystal-field admixing have been neglected. If, for example, noncubic second-order terms in the crystal-field potential are present at 77°K, they may cause significant admixing of closely spaced levels such as $^7F_1$ and $^7F_2$. Since a $J=2$ state is not connected by magnetic-dipole transitions from $^5D_0$, its addition into the original $^7F_1$ state would reduce the effective $^5D_0 \rightarrow {}^7F_1$ probability.

A comparison can also be made between the predicted and observed lifetimes of the $^5D_1$ state. We again assume the $^5D_1 \rightarrow {}^7F_2$ zero-phonon line is principally magnetic dipole with a probability given in

[11] This ratio varied from 0.54 to ~1.0 for crystals undergoing different heat treatment and annealing.

[12] F. Varsanyi, D. L. Wood, and A. L. Schawlow, Phys. Rev. Letters **3**, 544 (1959).

[13] See, for example, G. E. Peterson and P. M. Bridenbaugh, J. Opt. Soc. Am. **54**, 644 (1964).

Table IV. (Note that the relative intensities of $^5D_1 \rightarrow {}^7F_0$ and $^5D_1 \rightarrow {}^7F_2$ in Table III are approximately as predicted for magnetic-dipole radiation.) The ratio of zero phonon to vibrational sidebands for $^5D_1 \rightarrow {}^7F_2$ appeared about equal to that of $^5D_0 \rightarrow {}^7F_1$; however an accurate measurement was not possible. Since the $^5D \rightarrow {}_1{}^7F_4$, $^7F_5$, $^7F_6$ transitions were not identified in the fluorescence spectrum, being comparatively weak and possibly masked by transitions from $^5D_0$, we take, for the present estimate, their combined intensity to be equal to the total intensity of the other transitions in Table III. This yields a radiative lifetime of ≈ 0.6 msec; the observed $^5D_1$ lifetime is 0.1 msec at 77°K. Although the uncertainty associated with this estimate is large, it is not believed sufficient to account for more than a fraction of the above difference. Thus, it appears that the predominant decay of $^5D_1$ is nonradiative. That nonradiative transitions to $^5D_0$ are active is evident from the rate of the initial grown of the $^5D_0$ following selective excitation. Since nonradiative transitions from $^5D_0$ to ^7F_J were shown to be negligible, the same is probably also true for $^5D_1$.

Another measure of the ratio of radiative and nonradiative transitions from $^5D_1$ can be gotten from steady-state fluorescence intensities. Assume that the ion population $N(^5D_0)$ arises from a step-by-step cascade from the pump band via the intervening ^5D states in Fig. 1, the final step being the nonradiative transition $^5D_1 \rightarrow {}^5D_0$. From detailed balance,

$$N(^5D_0)\,W(^5D_0 \rightarrow {}^7F) = N(^5D_1)\,W^{\mathrm{NR}}(^5D_1 \rightarrow {}^5D_0), \quad (7)$$

where $W(^5D_0 \rightarrow {}^7F)$ is the total probability for decay from $^5D_0$, that is, $1/\tau(^5D_0)$. The fluorescence intensities I from $^5D_0$ and $^5D_1$, in terms of number of photons emitted, are related by

$$I(^5D_0)/[I(^5D_1)] = W^{\mathrm{R}}(^5D_0 \rightarrow {}^7F)\,N(^5D_0)/[W^{\mathrm{R}}(^5D_1 \rightarrow {}^7F)\,N(^5D_1)]. \quad (8)$$

Using Eq. (7) and the fact that the quantum efficiency for emission from $^5D_0$ is unity, i.e., $W(^5D_0 \rightarrow {}^7F) = W^{\mathrm{R}}(^5D_0 \rightarrow {}^7F)$, Eq. (8) reduces to

$$I(^5D_0)/[I(^5D_1)] = W^{\mathrm{NR}}(^5D_1 \rightarrow {}^5D_0)/[W^{\mathrm{R}}(^5D_1 \rightarrow {}^7F)]. \quad (9)$$

The experimentally observed intensity ratio, where the total $^5D_1$ intensity is estimated as above, is $\sim 13{:}1$. Comparison of the radiative and observed $^5D_1$ lifetimes yielded a ratio of nonradiative to radiative transition probabilities of 5:1 for Eq. (9).

The above difference may again be due in part to uncertainties in the relative intensity values. Another possibility, however, as noted previously in connection with the discussion of the transient fluorescence response of $^5D_0$, is that transitions from higher excited states may occur directly to $^5D_0$, in contrast to the assumptions made in deriving Eqs. (7) and (9). This would increase the emission from $^5D_0$ relative to that from $^5D_1$, thereby accounting for a larger ratio than expected from Eq. (9).

TEMPERATURE DEPENDENCE

The difference in the variations of the fluorescence lifetimes of $^5D_0$ and $^5D_1$ with temperature in Fig. 3 indicates that either the relative contribution of the temperature-dependent relaxation mechanism to the decay is significantly different for the two levels or different mechanisms are operative. The temperature dependence of fluorescence lifetimes can arise from several relaxation mechanisms, including thermal population of higher excited states which have different probabilities for radiative decay, vibronic transitions, and multiphonon nonradiative processes. The first possibility should be negligible in the present case because of the large separations of the ^5D_J levels with respect to kT. Vibronic transitions involving a single phonon frequency ν, where the range of frequencies and relative probability for inducing transitions is evident from the low-temperature vibronic spectrum, have a temperature dependence given by $\coth(h\nu/2kT)$. More generally, the intensity of an n-phonon overtone band varies from a constant at low temperatures, where $h\nu \ll kT$, to a T^n dependence at high temperatures. Multiple phonon combination bands involving sums and/or differences of various phonon frequencies also contribute to the over-all temperature dependence of the initial state lifetime. In $SrTiO_3$ the temperature dependence of vibronic band intensities is complicated by the fact that the frequencies of the lowest transverse optic branch vary as a function of temperature.[4]

Much of the temperature dependence of the $^5D_0$ lifetime appears to be attributable to the increased probability for vibronic transitions The intensity of a fluorescent transition in the usual steady-state limit of weak pumping is proportional to (1) the integrated absorption cross section of the pump band, (2) the lifetime of the fluorescent level, and (3) the radiative transition probability. If we include vibronic transitions under the definition of radiative probability, all of these factors may be temperature dependent. The probability for the purely radiative zero-phonon line, on the other hand, is considered to be essentially independent of temperature. This is observed for the $^5D_0 \rightarrow {}^7F_1$ transition where the intensity of the zero-phonon line exhibits little change with temperature between 77° and 295°K (the effects of decreasing $^5D_0$ lifetime may be partially cancelled by increasing pump absorption), whereas the vibrational sidebands on both the low- and high-energy sides grow with increasing temperature. Using the $^5D_0 \rightarrow {}^7F_1$ zero-phonon line intensity, which reflects any changes due to (1) and (2) above, as a comparison, it is found that for tempera-

TABLE V. Number and types of perturbed levels in a crystal field of O_h symmetry.

J	0	1	2	3	4	5	6
A_1	1	0	0	0	1	0	1
A_2	0	0	0	1	0	0	1
E	0	0	1	0	1	1	1
T_1	0	1	0	1	1	2	1
T_2	0	0	1	1	1	1	2

tures up to ~300°K the decrease in $^5D_0$ lifetime can be correlated with the increased intensity of the vibronic bands. Because the more rapid decrease in lifetime above 300°K was coupled with reduced fluorescence amplitude, further intensity measurements and correlations were not attempted.

Vibronic transitions are also evident in the fluorescence spectrum from $^5D_1$, the general structure associated with $^5D_1 \rightarrow {}^7F_2$ being similar to that for $^5D_0 \rightarrow {}^7F_1$. Selection rules for forced electric-dipole transitions from $^5D_1$ involving one phonon at various points in the Brillouin zone were determined as in Table III of Ref. 4. Of the points considered, all modes are allowed except for that transforming as Γ_2^- involving transitions to Γ_1^+. Thus, from the selection rules, the number of vibronic transitions from $^5D_1$ should be comparable to those from $^5D_0$, although the actual matrix elements and final intensities may be different. The contribution of vibronic transitions to the $^5D_1$ lifetime are small, however, and since the onset of the temperature-dependent decrease of the lifetime occurs at a lower temperature than for $^5D_0$, another temperature-dependent relaxation mechanism may be operative.

The results of the preceding section showed that the $^5D_1$ decay is predominantly nonradiative to $^5D_0$. Such transitions may arise from resonant energy transfer via ion–ion coupling[13] or multiphonon nonradiative processes. A possible mode for the former is a $^5D_1 \rightarrow {}^5D_0$ transition of one Eu^{3+} ion accompanied by an energy conserving $^7F_0 \rightarrow {}^7F_3$ transition of another, any small energy differences presumably being taken up by phonons. An argument against this mechanism is the low concentration of Eu, 0.03% (some of which is Eu^{2+}) and hence large interionic distance.[14]

TABLE VI. Number and types of perturbed levels in a crystal field of C_{4v} symmetry.

J	0	1	2	3	4	5	6
A_1	1	0	1	0	2	1	2
A_2	0	1	0	1	1	2	1
B_1	0	0	1	1	1	1	2
B_2	0	0	1	1	1	1	2
E	0	1	1	2	2	3	3

[14] Because of the requirement of some form of charge compensation for the substitution of Eu^{3+} into $SrTiO_3$, the Eu^{3+} ion distribution may not be random, however.

TABLE VII. Selection rules for electric-dipole transitions in C_{4v} symmetry.

	A_1	A_2	B_1	B_2	E
A_1	π				σ
A_2		π			σ
B_1			π		σ
B_2				π	σ
E	σ	σ	σ	σ	σ

The relative probabilities of large, multiphonon nonradiative transitions between different states arising from the dynamic orbit–lattice interaction are generally governed by selection rules and the amount of energy to be conserved. It has been recognized that the matrix elements of this interaction between free-ion states such as $^5D_0$ and $^5D_1$ are zero.[15,16] More generally, Orbach[17] pointed out that only those operators of the effective orbit–lattice interaction of order λ which satisfy the familiar triangle rule $|J-J'| \leq \lambda \leq |J+J'|$, where J and J' are the total angular-momentum quantum numbers of the two states, have nonzero matrix elements. Thus, for nonradiative transitions between ^5D_J states of Eu^{3+}, $^5D_1 \rightarrow {}^5D_0$ is forbidden, only second-order terms can contribute to $^5D_2 \rightarrow {}^5D_1$, $^5D_0$ and $^5D_3 \rightarrow {}^5D_0$, and both second- and fourth-order terms can contribute to $^5D_3 \rightarrow {}^5D_2$, $^5D_1$. There may, of course, be a partial breakdown of these rules due to admixing of states in a crystal. Nevertheless, they probably account for the fact that the $^5D_3$ and $^5D_2$ lifetimes are shorter than that for $^5D_1$ even though the energy gaps to the next lower level are larger, being ~3000 and ~2450 cm^{-1}, respectively, compared to ~1750 cm^{-1}. From the vibronic spectrum, lattice vibrational frequencies extend up to ≈800 cm^{-1} for the highest-frequency longitudinal optic branch; therefore several phonons are required to participate in any nonradiative transition attributed solely to phonon generation. The explicit temperature dependence of such processes can be derived if the form of the ion–lattice coupling and the number of active lattice or local mode vibrations and their frequency distributions are known.

TABLE VIII. Selection rules for magnetic-dipole transitions in C_{4v} symmetry.

	A_1	A_2	B_1	B_2	E
A_1		σ			π
A_2	σ				π
B_1				σ	π
B_2			σ		π
E	π	π	π	π	π

[15] E. Nardi and S. Yatsiv, J. Chem. Phys. **37**, 2333 (1962).
[16] J. D. Axe and P. P. Sorokin, Phys. Rev. **130**, 945 (1963).
[17] R. Orbach, Phys. Rev. **133**, A34 (1964).

A final temperature-dependent feature of the fluorescence properties of $SrTiO_3$:Eu^{3+} is the affect of the cubic→tetragonal structural phase transition[18] which occurs as the temperature is lowered below ≈110°K. Additional lines appear in the fluorescence spectrum which are interpreted as zero-phonon transitions of electric-dipole nature which became allowed in a nonspherically symmetric crystal-field environment. The intensity of these additional lines amounts to approximately 10%–15% of the fluorescence spectrum from $^5D_0$. The resulting change in the total radiative probability from $^5D_0$, which requires accurate correction for possible associated changes in the absorption cross section of the pump band, vibronic intensities, and lifetimes, was not determined. The change in the $^5D_0$ fluorescence lifetime in traversing the 110°K phase transition, however, was less than 10%, the detectable change being limited by experimental error.

SUMMARY

A comparison of the observed and predicted radiative lifetime of the $^5D_0$ level of Eu^{3+} in $SrTiO_3$ indicates that the decay arises from a combination of zero-phonon and phonon-assisted transitions, the latter accounting for much of the observed temperature dependence of the lifetime. Since at low temperatures there is no need to invoke the presence of nonradiative transitions to levels of the ^7F ground term, the quantum efficiency for total emission from $^5D_0$ is unity. The decay from $^5D_1$ consists of radiative transitions to ^7F and more probable nonradiative transitions to $^5D_0$. Decays from $^5D_2$ and $^5D_3$ are very fast and predominantly nonradiative, possibly reflecting the greater probability for multiphonon nonradiative transitions with respect to the forbidden $^5D_1 \rightarrow {}^5D_0$ transition. Energy from higher excited states decays to $^5D_0$ via step-by-step cascade involving intervening ^5D_J levels together with evidence of some direct transitions which bypass $^5D_1$.

ACKNOWLEDGMENTS

We would like to express our thanks to Miss Marilyn Harrison for computational assistance and Mr. Paul Kocincki and Mr. Thomas Varitimos for experimental assistance.

APPENDIX

The irreducible representations of crystal-field levels and the selection rules and polarization (π, σ) for electric-dipole and magnetic-dipole transitions for cubic (O_h) and tetragonal (C_{4v}) rare-earth site symmetries are given below in Tables V–VIII.

In a cubic field, electric-dipole transitions are forbidden; magnetic-dipole transitions (unpolarized) are allowed between A_1–T_1, A_2–T_2, E–T_1T_2, T_1–$A_1ET_1T_2$, and T_2–$A_2ET_1T_2$.

[18] See the recent paper by F. W. Lytle [J. Appl. Phys. **35**, 2212 (1964)] and references therein to earlier studies of this phase transition.